

## The effect of growth condition on the structure of 2H–AlN films deposited on Si(111) by plasma-assisted molecular beam epitaxy

U. Kaiser<sup>a)</sup>

*Institut für Festkörperphysik, Friedrich-Schiller-Universität Jena, Max-Wien-Platz 1, D-07743 Jena, Germany*

P. D. Brown

*Department of Materials Science and Metallurgy, University of Cambridge, Pembroke Street, CB2 3QZ Cambridge, United Kingdom*

I. Khodos

*Institute of Microelectronics Technology and High Purity Materials RAS, 142432 Chernogolovka, Russia*

C. J. Humphreys

*Department of Materials Science and Metallurgy, University of Cambridge, Pembroke Street, CB2 3QZ Cambridge, United Kingdom*

H. P. D. Schenk and W. Richter

*Institut für Festkörperphysik, Friedrich-Schiller-Universität Jena, Max-Wien-Platz 1, D-07743 Jena, Germany*

(Received 20 April 1998; accepted 14 December 1998)

The effects of substrate cleaning, nitridation time, and substrate temperature in the range 800–1000 °C on the microstructure of AlN/Si(111) films grown by simultaneous plasma-assisted molecular beam epitaxy have been investigated. It has been demonstrated, using a combination of conventional and high-resolution transmission electron microscopy, that the interface structure, the film defect structure, and the film surface roughness are strongly related. The formation of single crystal 2H–AlN films with atomically flat surfaces occurs at 800 °C for conditions of 2.5 nm/min growth rate on very pure, atomically flat Si substrates.

### I. INTRODUCTION

Aluminum nitride is of considerable interest for high-power, high-temperature, and radiation-resistant electronic and optoelectronic applications.<sup>1</sup> In combination with other group III–V nitrides, AlN is viewed as a promising material for semiconductor device applications at blue and ultraviolet wavelengths. Thin layers of wurtzite of AlN (basal plane lattice parameters,  $a = 0.3112$  nm) have become widely used as a buffer layer between various substrates and deposited GaN or SiC films to improve their structural quality and electronic properties.<sup>2–7</sup> Thick AlN layers also have application in surface acoustic wave (SAW) devices because of the high velocity of acoustic waves in this material.<sup>6</sup>

The well-known fact that defect microstructure is strongly related to the properties of semiconductors stimulates attempts to grow AlN films of high structural

perfection. Highest quality AlN films were obtained using 6H–SiC substrates<sup>8–10</sup> (basal plane lattice parameter,  $a = 0.308$  nm) because of the relatively small lattice mismatch (0.9%) and an identical film/substrate crystallographic relationship.<sup>11</sup> It was shown<sup>9,10</sup> also that the quality of the thicker AlN films was strongly influenced by the precise orientation of the substrate surface.

Unfortunately, the large lattice mismatch between AlN and the more widely used Si ( $a = 0.5430$  nm) and sapphire ( $a = 0.4758$  nm) substrates leads to the formation of a high density of threading defects in the AlN film which may have consequence for the performance and lifetime of device structures. According to Dovidenko *et al.*,<sup>12</sup> The structure of AlN films grown by metalorganic chemical vapor deposition on silicon and sapphire substrates was found to be highly textured  $c$ -axis oriented. High temperature deposition of AlN films by reactive sputtering in high vacuum on Si(111) substrates results in highly  $c$ -axis, preferred-orientation polycrystalline wurtzitic growth.<sup>13,14</sup> Using the molecular beam epitaxy (MBE) technique and growing on Si(111), AlN films with a rough interface and an average surface

<sup>a)</sup>Address all correspondence to this author.  
e-mail: kaiser@pinet.uni-jena.de

roughness (rms) of 48 nm were obtained by Sanchez-Garcia *et al.*,<sup>20</sup> while a sharp interface between the AlN layer and Si(111) was reported by Bourret *et al.*<sup>21</sup>

The processing of substrate surfaces is of great importance for the subsequent nucleation and growth of high quality films. For the case of AlN/Si, controlled exposure of the substrate to a nitrogen plasma before the start of layer growth activates surface reactions which define a suitable template for continued layer growth. Similarly, the process of nitridation is generally used to prepare sapphire and GaAs substrates, prior to the deposition of III-V nitrides, with the formation of thin AlN<sup>6</sup> and GaN layers, respectively.<sup>15</sup> Indeed, the nitridation of a substrate surface can hardly be avoided when using a plasma enhanced deposition technique for nitride growth. To the best of our knowledge, a time-controlled study of the nitridation of Si has not been reported to date.

This work is primarily concerned with the influence of substrate cleaning procedures and nitridation time on the initial formation and subsequent evolution of crystalline AlN thin films. In addition, we report on the influence of a range of growth parameters, including substrate temperature and growth rate, on the quality of the AlN overlayers, as examined using a combination of conventional and high resolution transmission electron microscopy (TEM) and atomic force microscopy (AFM).

## II. EXPERIMENTAL

AlN films were grown on Si(111) substrates by MBE using thermally evaporated aluminum and an rf-plasma excited nitrogen gas as described fully elsewhere.<sup>16</sup> Two different *ex situ* processes of wet chemical cleaning of the Si-substrate were compared, first according to the modified RCA method<sup>17</sup> and second after Ishizaka and Shiraki.<sup>18</sup> The latter cleaning method will be called the Shiraki method in this paper. The main difference between these two methods is that after the RCA process the Si surface is hydrogen-terminated, whereas the Shiraki method produces an oxygen passivation. In contrast to the hydrogen termination, the oxygen termination is completely removable by substrate heating at the substrate temperatures used. Substrates were held at the growth temperature and then exposed to a flow of activated nitrogen from the plasma source for varying times before the shutter of the aluminum evaporator was opened and layer growth initiated. For all samples a flux rate ratio of Al/N close to 1:1 was established. The influence of substrate temperature in the range 800 up to 1000 °C and that of growth rate from 1 to 5.5 nm/min were examined. The surface topography and rms-roughness of the films were investigated using AFM under ambient conditions in contact mode. Samples for TEM examination both in plan view and cross

section were prepared using standard techniques and investigated using JEOL JEM-1200, JEM-2000FX, and JEM-4000EX transmission electron microscopes.

## III. RESULTS AND DISCUSSION

### A. Growth on RCA cleaned substrates

An AlN film was grown at 1000 °C on an RCA cleaned Si(111) substrate nitrided for 300 s before growth (specimen 1, Table I). As shown in Fig. 1, the resultant deposit comprises columnar AlN grains. The AlN grains visible in strong contrast are generally loosely spaced [Fig. 1(a)]. No evidence for Si between adjacent crystalline AlN columns was found by EDX measurements. The amorphous-like contrast seen in Fig. 1(b) between adjacent grains is presumed to arise from AlN columns which are far from the Bragg position. The higher magnified image of Fig. 1(c) recorded at the epilayer/substrate interface shows a rough substrate surface, an ~5 nm thick amorphous layer between the Si substrate and the AlN overlayer, and a thin transition zone with the formation of small misoriented grains in the very early stages of growth. Misorientation of these small interfacial grains is associated with the roughness at the substrate surface. An amorphous Si<sub>3</sub>N<sub>4</sub> layer is presumed to be created at the interface following the reaction of Si with nitrogen. The columnar grains are strongly oriented with the *c*-axis in the growth direction, i.e., with [0002]AlN || [111]Si, as demonstrated by the [110] selected area diffraction pattern of Fig. 1(d) which covers an area of about 20 μm<sup>2</sup> at the interface. However, there are huge misorientations in the plane of growth of about 30° as shown by diffraction patterns recorded from a plan-view sample foil [Fig. 1(e)]. The grain size is typically 110 nm and the upper surface is strongly faceted [Fig. 1(a)]. The AFM image of the resultant growth surface [Fig. 2(a)] additionally demonstrates that some grains are randomly elongated in the *c*-plane. A high rms-roughness of 8 nm for this 1000 × 1000 nm area was found.

Using the same nitridation time of 300 s prior to growth and decreasing the growth temperature to 800 °C (specimen 2) led to the formation of a similar columnar structure to that of Fig. 1, with an ~5 nm thick amorphous layer still being present at the epilayer/substrate interface. Considerable in-plane misorientation of the growth columns was again observed, with an even larger misorientation for a 100 nm layer of faulted material adjacent to the substrate. The columnar grains shown in the AFM image of Fig. 2(b) are all about the same size of 75 nm diameter. Both grain size and layer roughness have decreased as compared with the growth at 1000 °C (Table I).

A shorter 60 s nitridation time (specimen 3), using the same growth temperature of 800 °C, acted to pro-

TABLE I. Growth parameters and summary of results for a range of AlN films grown on Si(111) by plasma-assisted MBE.

	Specimen 1	Specimen 2	Specimen 3	Specimen 4	Specimen 5	Specimen 6
Substrate cleaning	RCA	RCA	RCA	RCA	Shiraki	Shiraki
Substrate temp. (°C)	1000	800	800	800	800	850
Nitridation time (s)	300	300	60	10	10	10
Growth rate (nm/min)	1	1	1	5.5	2.5	2.5
Thickness of amorphous layer (nm)	4–6	5	2–3	~1, partial coverage	0	0
Layer microstructure	Columnar grains	Columnar grains	Columnar grains	Epitaxial	Threading dislocations and growth hillocks	Threading dislocations, growth hillocks, and platelets
Orientation relationship	<i>c</i> -axis oriented along the growth direction; misorientation in the growth plane	<i>c</i> -axis oriented along the growth direction; misorientation in the growth plane	[0001]AlN    [111]Si and [1 $\bar{2}$ 10]AlN    [110]Si, small misorientation in growth plane	[0001]AlN    [111]Si and [1 $\bar{2}$ 10]AlN    [110]Si	[0001]AlN    [111]Si and [1 $\bar{2}$ 10]AlN    [110]Si	[0001]AlN    [111]Si and [1 $\bar{2}$ 10]AlN    [110]Si
Mean grain size (nm)	110	75	40	80	Single crystal	Single crystal
rms-roughness (nm) <sup>a</sup>	8	5	6	4	0.25	0.4
Layer surface	Faceted	Faceted	Faceted	Faceted	Very flat with a few hillocks	Very flat with some hillocks
Void formation	No	No	No	No	A few big voids	Many small voids

<sup>a</sup>rms-roughnesses were determined from  $1 \times 1 \mu\text{m}$  precipitate and hillock-free regions using AFM.

duce a more homogeneous AlN layer [Fig. 3(a)], although a narrow amorphous layer was still identified at the epilayer/substrate interface [Fig. 3(b)]. Diffraction patterns recorded from a plan-view foil using the same selected area aperture as before confirmed that the in-plane misorientations had significantly decreased [Fig. 3(c)]. Diffraction patterns recorded from a cross-sectional specimen confirmed the same [0002]AlN || [111]Si epitaxial relationship [Fig. 3(d)]. The surface roughness of the layer had similarly decreased and the average grain size was smaller [Fig. 2(c)] as compared with specimens 1 and 2, as determined using AFM.

In an attempt to eliminate the amorphous intermediate layer, the substrate was nitridated for only 10 s prior to the initiation of growth (specimen 4). The resulting structure, also grown at a higher growth rate of 5.5 nm/min, is shown in Fig. 4. In this instance a very thin discontinuous amorphous layer was present. Diffraction patterns confirmed a strong epitaxial relationship between the epilayer and substrate [Figs. 4(c) and 4(d)]. As seen in the weak-beam dark-field image in Fig. 4(a),

there is a very high density of threading dislocations which self-annihilate and decrease in density as the film gets thicker. Investigation from tilted weak beam plan-view samples confirmed that growth columns were delineated by low-angle grain boundaries comprising mixed character threading dislocations, similar to the results reported by Xin *et al.*<sup>19</sup> for GaN on  $\{\bar{1}\bar{1}\bar{1}\}$ B GaAs. The surface of the layer is still rather rough and faceted [Fig. 4(a)] as also shown by AFM [Fig. 2(d)]. By comparison of specimens 3 and 4 it can be concluded that the epitaxy becomes better when the amorphous layer gets thinner. The different growth rate does not affect the resultant layer defect microstructure significantly; therefore the structural changes are assumed to be mostly determined by the influence of substrate nitridation time.

The profound difference in the AlN layer microstructure grown at 1000 and 800 °C is probably caused by the increases of the mobility of adatoms at elevated substrate temperature. This promotes the formation of homogeneous single crystalline columns with large grain size but low packing density.

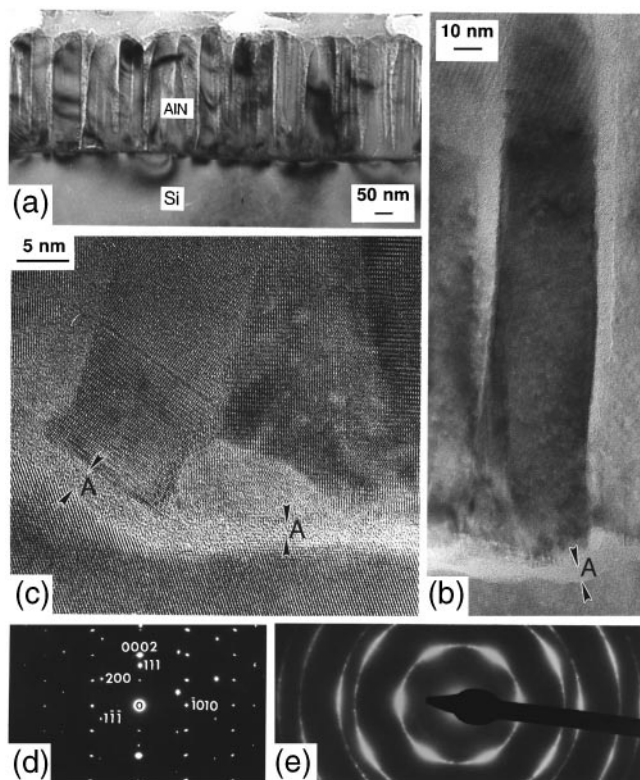


FIG. 1. (a) Cross-sectional TEM micrographs of the AlN layer grown at 1000 °C and 300 s nitridation time showing columnar layer structure and a faceted layer surface. This image was taken in an underfocus condition using the Fresnel contrast to enhance the visibility of space between the columns. In (b) the high-resolution TEM image taken in the [110] direction of Si shows amorphous-like contrast between columns. (c) High-resolution TEM image showing misoriented grains in the initial stage of growth and thick amorphous interface as arrowed by "A." (d) and (e) are SAD patterns in cross section and plan view, respectively, demonstrating a good *c*-axis orientation and a strong in-plane misorientation.

The exposure of the Si substrate to activated nitrogen before Al exposure leads to a reaction between the silicon and nitrogen causing the formation of an amorphous layer presumed to be  $\text{Si}_3\text{N}_4$  of about 5 nm thickness as observed after 300 s of nitridation. This interlayer is probably responsible for the misorientation of the columns in the plane of growth, in view of the lack of registry with the original Si(111) substrate. Although it was not possible to completely remove the amorphous interlayer, a discontinuous amorphous layer was remnant for the very shortest nitridation times used, and its influence on the evolution of the AlN deposit was considerably reduced. The implication here is that seeded growth has occurred to retain strong epitaxial relationship with the substrate. It should be noted that the rms roughness of an area of  $1000 \times 1000$  nm of the substrate was found to be 2.0 nm after RCA cleaning (measured before deposition), giving rise to the faceted AlN layer surfaces which were always observed using

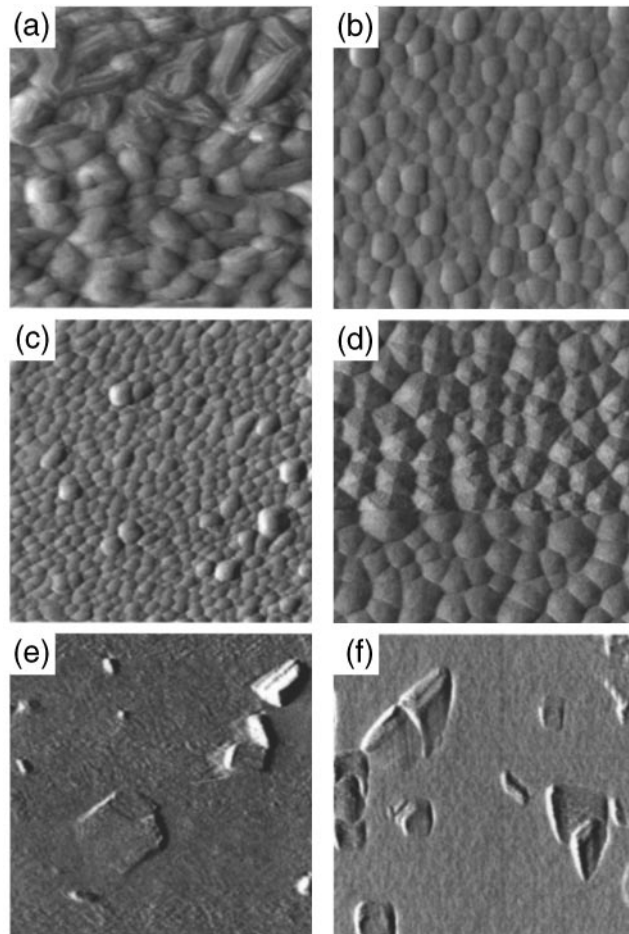


FIG. 2. Plan-view AFM micrographs (a) and (f) corresponding to specimens 1 to 6. In (a), (b), (c), (e), and (f) the size of the scanned area is  $1 \times 1 \mu\text{m}$ . In (d) it is  $500 \times 500$  nm where a higher resolution was achieved in the upper part of the image where the grain facets are clearly resolved.

this cleaning method. The rms roughnesses of the AlN layer achieved on these substrates are in the range of 5 nm which is similar or slightly below that reported by other workers.<sup>20,23</sup>

## B. Growth on substrates cleaned with the Shiraki method

We now report on the influence of an alternative Si substrate cleaning method<sup>18</sup> on the structure of the AlN films (specimens 5 and 6). The Si substrate surface roughness measured over an area of  $1000 \times 1000$  nm was reduced by a factor of 5 to 0.4 nm, as compared with Si cleaned using the RCA method. The remnant oxide on the Si-surface after applying the Shiraki cleaning method will be easily desorbed during substrate heating up to 900 °C before deposition as distinct from the RCA cleaned material where a hydrogen termination layer will still passivate the Si-surface at the growth temperatures used. Growth on Shiraki-cleaned substrates

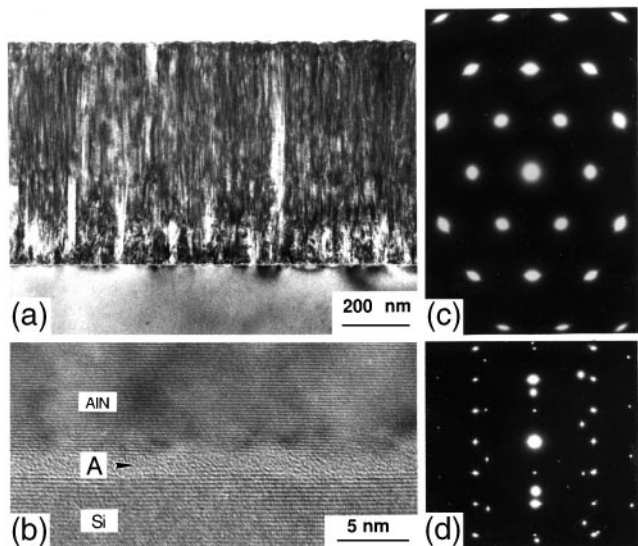


FIG. 3. (a) TEM bright-field micrograph of a cross section of specimen 3 formed at 800 °C and 60 s nitridation time showing strain at the interface, a transition region of about 100 nm layer thickness, and a faceted layer surface. In (b) the amorphous region of about 2 nm thickness between the Si substrate and the AlN layer is shown in high resolution in the [110] direction of Si. In (c) and (d) the plan view and cross section diffraction patterns demonstrate a good *c*-axis and in-plane orientation.

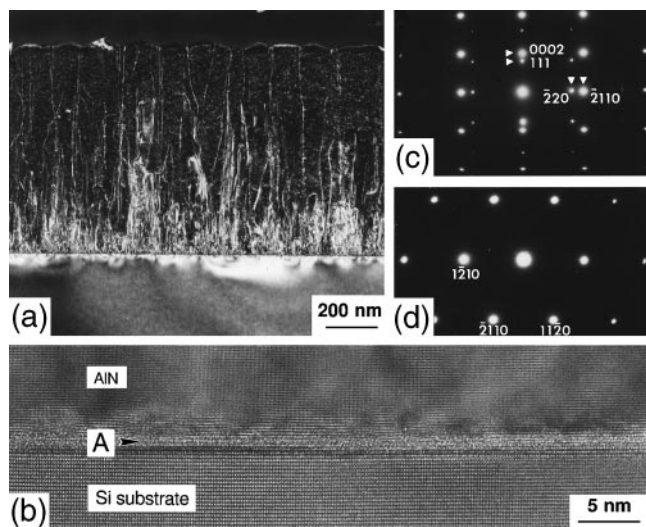


FIG. 4. (a) Dark-field micrograph of AlN (specimen 4) formed at 800 °C with 10 s nitridation time. Most threading dislocations visible are of mixed type, and their density is much higher in a transition zone of about 200 nm thickness than in the subsequent part of the layer. A high-resolution TEM micrograph taken at the [112] zone of Si is seen in (b) showing that no continuous amorphous interface region (marked at A) is present. The SAD patterns in (c) and (d) show that the layer is epitaxial to the substrate.

at 800 °C after an *in situ* nitridation time of 10 s resulted in a single crystalline layer which exhibited a well-defined epilayer/substrate interface as seen from the high-resolution TEM image of Fig. 5(a) free of any

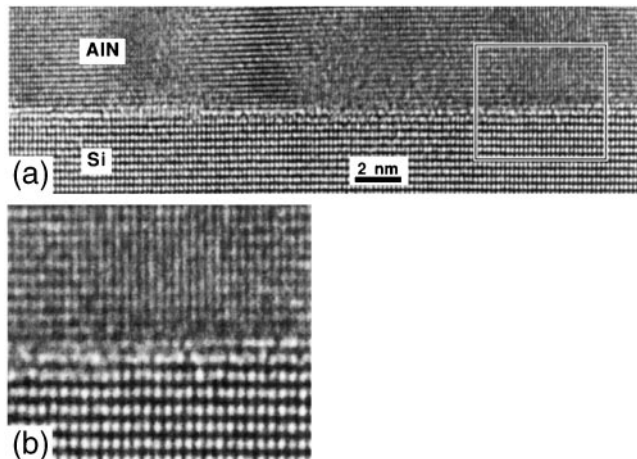


FIG. 5. (a) High-resolution TEM micrograph of the Si/AlN interface region of specimen 5 (see Table I) observed along the Si[112] axis showing the flatness of the interface region and the absence of an amorphous layer. The marked area is shown in more detail in (b), demonstrating the lattice parameter fit of  $4a_{Si}$  to  $5a_{AlN}$  in most cases.

amorphous interlayer. The Si substrate is predominantly atomically flat with some bilayer steps, as seen in more detail in Fig. 5(b). The transition between Si and AlN is very sharp in agreement with results recently reported by Bourret *et al.*<sup>21</sup> It was determined from Fig. 5(b) that the lattice parameter condition of  $4a_{Si} - 5a_{AlN}$  is fulfilled along the whole interface in accordance with the calculated ratio of 0.76 for 022 Si and  $\bar{2}110$  AlN fringes, implying a periodic array of interfacial misfit dislocations.

Another striking feature of the structure of specimen 5 is the extremely flat epilayer surface [Fig. 6(a)], with a roughness of only 1–2 atomic layers [e.g., background of Fig. 2(e)]. Although a small number of regions exhibit hillock structures which are the same as in specimen 6 [e.g., Fig. 7(a), features denoted F], it is not clear whether these hillocks and the corresponding features seen in the plan-view AFM image of Fig. 2(e) are the same (this question is presently under further investigation). The main defects within this single crystal epilayer are threading dislocations of mixed character. However, it should be noted that voids are present in the Si substrate just underneath the epilayer [Fig. 6(b)]. The highly magnified image of Fig. 6(d) shows clearly that the void is bounded by amorphous material. The adjacent crystalline Si substrate and AlN layer are indicated. It is interesting to note that the line of the original epilayer/substrate interface is retained above this void which discounts the possibility of etching of the substrate prior to growth (otherwise the void would become filled in). In addition, these voids are visible in the light microscope after the deposition; therefore it is not possible that they were created during TEM specimen preparation. However, no remarkable evidence for Si was found in the layer using

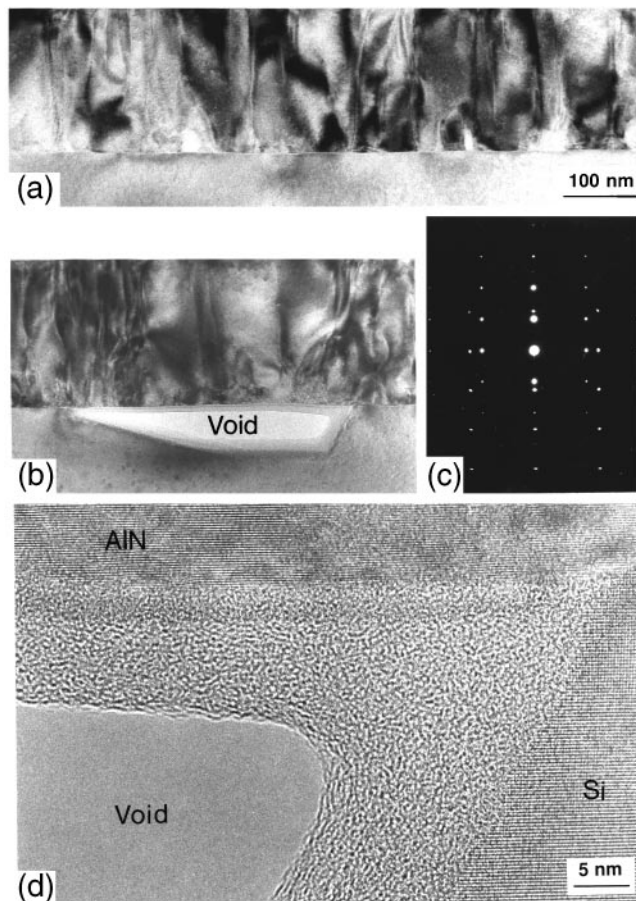


FIG. 6. Bright-field TEM images of specimen 5 grown at 800 °C (see Table I) showing in (a) a very homogeneous single crystalline AlN film [see diffraction pattern in (c)] with an extremely flat layer surface corresponding to the atomically flat sharp interface as seen in Fig. 5. In (b) a void is shown which apparently appears in the Si substrate. (d) shows a high-resolution TEM image obtained along the [112] axis of Si showing the void of (b) and demonstrates that it is surrounded by amorphous material.

EDX analysis, so the implication is that Si is lost from the substrate, has presumably diffused through the layer, and become desorbed from the growth surface (work is continuing to clarify this remarkable observation).

Growing at a higher substrate temperature of ~850 °C but otherwise under the same growth conditions (specimen 6) leads to the appearance of a higher density of smaller voids in the substrate as well as to greater extent of hillock formation [Figs. 7(a) and 7(c)] in the AlN film. The hillocks are single crystal, spread through the whole epilayer, and form “caps” on the surface. The AFM image of the surface of specimen 6 [Fig. 2(f)] also shows the combination of a high density of hillocks and a high background flatness of the layer surface. It is noted that these hillocks are sometimes connected with the location of voids under the AlN layer in the Si substrate (Figs. 7(a) and 7(c)]. The features marked at V in Fig. 7(a) are possibly voids in the initial

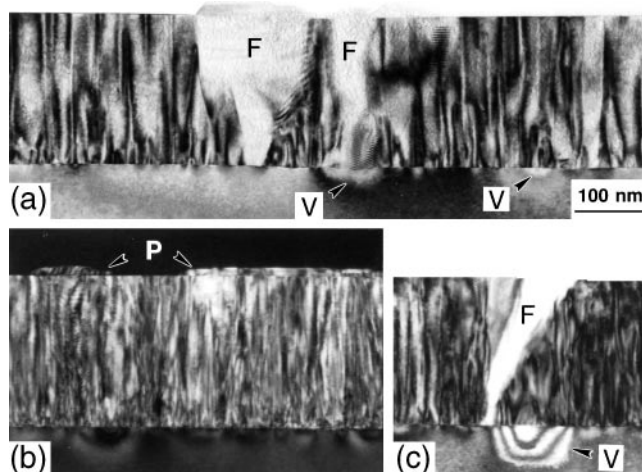


FIG. 7. Bright-field and dark-field TEM images of specimen 6 grown at 850 °C showing a homogeneous single crystalline layer with different kinds of defects as hillocks, marked “F” in (a) and (c), voids marked “V” in (c) and (a), and precipitates marked as “P” in (b).

stage of formation. However, as was again confirmed by EDX analysis, the hillocks do not contain Si, and their Al content was found not to differ from the Al content of the entire layer (it was not possible to investigate the nitrogen content using our x-ray detector). Indeed, both plan-view and cross-sectional investigations suggested that the hillocks comprise the same phase of AlN. It is interesting to note that misorientation between 0001 directions of the hillocks and the film is quite large up to 35°. Void formation in the first instance is possibly associated with the high stress between the layer and the substrate. This observation is similar to the void formation found in SiC/Si,<sup>22</sup> where voids start to grow at substrate defects, thereby enhancing the diffusion of Si along layer defects. In specimens 1 to 4 (Table I), interfacial stresses were reduced by the presence of an amorphous interlayer, and no voids were observed.

In addition, the AlN layer surfaces grown on Shiraki-cleaned substrates sometimes exhibit flat platelike crystals, denoted by P in Fig. 7(b), delineating a well-defined interface with the epilayer growth surface. Using EDX analysis it was found that such platelike crystals on top of the AlN layer do contain Si. Dark-field cross-sectional images obtained using Si reflections show similar contrast from the Si substrate and the platelike crystals. Therefore we may draw the conclusion that these platelike crystals are single crystalline Si. This is similar to the observation of single crystalline Si on top of a SiC layer grown on Si(111) which exhibit voids in the substrate.<sup>22</sup> However, the shape of these Si platelets was different for the case of SiC growth, reflecting their different registry with the growth surface lattice.

The absence of an amorphous layer for single crystal AlN layers grown on O-terminated Si substrates prepared

using the Shiraki method is attributed to the highly clean substrate surface. As activated nitrogen is always present in the vacuum chamber, a very short nitridation time of about 10 s prior to the growth is required to achieve reproducible, well-defined substrate surfaces and does not in this case result in the formation of an amorphous  $\text{Si}_3\text{N}_4$  layer. The fact that an epitaxial single crystalline layer is grown showing an atomically flat surface is strongly connected with a pure and flat substrate surface. Moreover, it might be possible that the polarity of the AlN pair is changed in the way that now the upper surface is Al terminated instead of probably N termination when growing on an amorphous  $\text{Si}_3\text{N}_4$  interface layer (future work will be addressed to that problem and the results of these investigations will be described in due course). Two-dimensional AlN growth by MBE can occur, as distinct from the three-dimensional growth which characterized the layers formed on an amorphous template following RCA cleaning. The appearance of voids, hillocks, and platelike crystals seems to be strongly associated and are probably connected to the lack of an amorphous layer and the growth on a flat, clean Si substrate surface. Strain enhanced Si diffusion from the substrate can take place under such conditions. Moreover, because of the high solubility of Si in Al,<sup>24</sup> voids may start to form as soon as Al contacts the substrate. Further investigations are in progress to characterize this process more fully.

#### IV. SUMMARY

The influence of the nitridation time prior to deposition and the effect of two different Si substrate cleaning methods on the microstructural development of AlN films grown by MBE have been described. The growth has been found to be highly sensitive to the Si substrate cleaning procedure used, growth temperature, and the extent of nitridation for the case of growth on RCA cleaned substrates. Optimum growth conditions were found to be 800 °C substrate temperature, 2.5 nm growth rate, and the exposure of nitrogen flux for 10 s before deposition. Using RCA cleaned substrates, epitaxial columnar growth is present whereas the optimum growth of single crystalline hexagonal AlN occurs on clean, atomically flat Si surfaces which were achieved by the Shiraki cleaning method only. Work to address and suppress the problem of void and hillock formation during growth on Shiraki-cleaned substrates is continuing.

#### ACKNOWLEDGMENTS

The authors acknowledge the financial support of this research by the British-German ARC program (No. 313-ARC-VII), the Sonderforschungsbereich 196

(No. A03), and the Newton Trust (Cambridge), and we thank Dr. Martin Albrecht for stimulating discussions. We also thank Mr. J. Jinschek and Mrs. H. Walther for help in specimen preparation and Mr. J. Schulze and Mr. J. Jinschek for AFM measurements.

#### REFERENCES

1. M. Katayama, T. Fukui, T. Shiosaki, and A. Kawabata, *Jpn. J. Appl. Phys.* **22**, 139 (1982).
2. H. Amano, N. Sawaki, I. Akasaki, and Y. Toyoda, *J. Appl. Phys. Lett.* **48**, 353 (1986).
3. F. A. Ponce, B. S. Krusor, J. S. Mayor, W. E. Plano, and D. F. Welch, *Appl. Phys. Lett.* **67**, 410 (1995).
4. T. W. Weeks, M. D. Bremser, K. S. Ailey, E. Carlson, W. G. Perry, and R. F. Davis, *Appl. Phys. Lett.* **67**, 401 (1995).
5. S. Tanaka, S. Iwai, and Y. Aoyagi, *J. Cryst. Growth* **170**, 329 (1997).
6. O. Ambacher, R. Dimitrov, D. Lentz, T. Metzger, W. Rieger, and M. Stutzman, *J. Cryst. Growth* **170**, 335 (1997).
7. I. Akasaki, H. Amano, Y. Koide, K. Hiramoto, and N. Sawaki, *J. Cryst. Growth* **98**, 209 (1989).
8. A. Taylor and R. M. Jones, *Silicon Carbide, A High Temperature Semiconductor*, edited by J. R. O'Connor and J. Smittens (Pergamon Press, New York, 1960), p. 147.
9. S. Tanaka, R. S. Kern, J. Bentley, and R. F. Davis, *Jpn. J. Appl. Phys.* **35**, 1641 (1996).
10. R. F. Davis, S. Tanaka, and R. S. Kern, *J. Cryst. Growth* **163**, 93 (1996).
11. S. Stemmer, P. Pirouz, Y. Ikuhara, and R. F. Davis, *Phys. Rev. Lett.* **77**, 1797 (1996).
12. K. Dovidenko, S. Oktyabrsky, and J. Narayan, *J. Appl. Phys.* **79**, 2439 (1996).
13. W. J. Meng, J. A. Sell, and T. A. Perry, *J. Appl. Phys.* **75**, 3446 (1994).
14. I. Ivanov, L. Hultman, K. Järrendahl, P. Mårtensson, J. E. Sundgren, B. Hjörvarsson, and J. E. Greene, *J. Appl. Phys.* **78**, 5721 (1995).
15. M. Mutoh, P. O'Keefe, S. Den, S. Kumuro, T. Morikawa, Y. J. Park, K. Hara, H. Muneke, and H. Kukimoto, *Appl. Surf. Sci.* **113**, 622 (1997).
16. S. Karmann, H. P. D. Schenk, U. Kaiser, A. Fissel, and W. Richter, *Mater. Sci. Eng.* (in press).
17. S. Kern and D. A. Pustinen, *RCA Rev.* **31**, 197 (1970).
18. I. Ishizaka and Y. Shiraki, *J. Electrochem. Soc.* **133**, 666 (1986).
19. Y. Xin, P. D. Brown, T. S. Cheng, C. T. Foxon, and C. J. Humphreys, *Inst. Phys. Conf. Ser.* **157**, 95 (1997).
20. A. Sánchez-García, E. Calleja, E. Monroy, F. Sánchez, F. Calle, E. Muñoz, A. Sanz-Hervás, C. Villar, and M. Aguilar, *MRS Internet J. Nitride Semiconductor Research* **2**, 33 (1998).
21. A. Bourret, A. Barski, J. L. Rouviere, G. Renaud, and A. Barbier, *J. Appl. Phys.* **83**, 4 (1998).
22. U. Kaiser, S. B. Newcomb, M. W. Stobbs, M. Adamik, A. Fissel, and W. Richter, *J. Mater. Res.* **13**, 3571–3579 (1998).
23. F. Malengreau, M. Vermeersch, S. Hagège, R. Sporken, M. D. Lange, and R. Caudano, *J. Mater. Res.* **12**, 175 (1997).
24. R. Bergmann, J. Kühne, H. Werner, S. Oelting, M. Albrecht, H. P. Strunk, K. Herz, and M. Powalla, *IEEE First World Conference on Photovoltaic Energy Conversion*, Hawa 1994 (IEEE Publishing Service, New York 1994), p. 1398.